Editors' Suggestion | Featured in Physics

Improved Constraints on Sterile Neutrino Mixing from Disappearance Searches in the MINOS, MINOS+, Daya Bay, and Bugey-3 Experiments

P. Adamson,[δ,1] F. P. An,[δ,2] I. Anghel,[μ,3] A. Aurisano,[μ,4] A. B. Balantekin,[δ,5] H. R. Band,[δ,6] G. Barr,[μ,7] M. Bishai,[δ,8] A. Blake,[μ,9,10] S. Blyth,[δ,11] G. F. Cao,[δ,12] J. Cao,[δ,12] S. V. Cao,[μ,13] T. J. Carroll,[μ,13] C. M. Castromonte,[μ,14] J. F. Chang,[δ,12] Y. Chang,[δ,15] H. S. Chen,[δ,12] R. Chen,[μ,16] S. M. Chen,[δ,17] Y. Chen,[δ,18,19] Y. X. Chen,[δ,20] J. Cheng,[δ,12] Z. K. Cheng,[δ,19] J. J. Cherwinka,[δ,5] S. Childress,[μ,1] M. C. Chu,[δ,21] A. Chukanov,[δ,22] J. A. B. Coelho,[μ,23] J. P. Cummings,[δ,24] N. Dash,[δ,12] S. De Rijck,[μ,13] F. S. Deng,[δ,25] Y. Y. Ding,[δ,12] M. V. Diwan,[δ,8] T. Dohnal,[δ,26] D. Dolzhikov,[δ,22] J. Dove,[δ,27] M. Dvořák,[δ,12] D. A. Dwyer,[δ,28] J. J. Evans,[μ,16] G. J. Feldman,[μ,29] W. Flanagan,[μ,13,30] M. Gabrielyan,[μ,31] J. P. Gallo,[δ,32] S. Germani,[μ,33] R. A. Gomes,[μ,14] M. Gonchar,[δ,22] G. H. Gong,[δ,17] H. Gong,[δ,17] P. Gouffon,[μ,34] N. Graf,[μ,35] K. Grzelak,[μ,36] W. Q. Gu,[δ,8] J. Y. Guo,[δ,19] L. Guo,[δ,17] X. H. Guo,[δ,37] Y. H. Guo,[δ,38] Z. Guo,[δ,17] A. Habig,[μ,39] R. W. Hackenburg,[δ,8] S. R. Hahn,[μ,1] S. Hans,[δ,8,*] J. Hartnell,[μ,40] R. Hatcher,[μ,1] M. He,[δ,12] K. M. Heeger,[δ,6] Y. K. Heng,[δ,12] A. Higuera,[δ,41] A. Holin,[μ,33] Y. K. Hor,[δ,19] Y. B. Hsiung,[δ,11] B. Z. Hu,[δ,11] J. R. Hu,[δ,12] T. Hu,[δ,12] Z. J. Hu,[δ,19] H. X. Huang,[δ,42] J. Huang,[μ,13] X. T. Huang,[δ,43] Y. B. Huang,[δ,12] P. Huber,[δ,44] D. E. Jaffe,[δ,8] K. L. Jen,[δ,45] X. L. Ji,[δ,12] X. P. Ji,[δ,8] R. A. Johnson,[δ,46] D. Jones,[δ,47] L. Kang,[δ,48] S. H. Kettell,[δ,8] L. W. Koerner,[μ,41] S. Kohn,[δ,49] M. Kordosky,[μ,50] M. Kramer,[δ,28,49] A. Kreymer,[μ,1] K. Lang,[μ,13] T. J. Langford,[δ,6] J. Lee,[δ,28] J. H. C. Lee,[δ,51] R. T. Lei,[δ,48] R. Leitner,[δ,26] J. K. C. Leung,[δ,51] F. Li,[δ,12] H. L. Li,[δ,12] J. J. Li,[δ,17] Q. J. Li,[δ,12] S. Li,[δ,48] S. C. Li,[δ,44] S. J. Li,[δ,19] W. D. Li,[δ,12] X. N. Li,[δ,12] X. Q. Li,[δ,52] Y. F. Li,[δ,12] Z. B. Li,[δ,19] H. Liang,[δ,25] C. J. Lin,[δ,28] G. L. Lin,[δ,45] S. Lin,[δ,48] J. J. Ling,[δ,19] J. M. Link,[δ,44] L. Littenberg,[δ,8] B. R. Littlejohn,[δ,32] J. C. Liu,[δ,12] J. L. Liu,[δ,53] Y. Liu,[δ,43] Y. H. Liu,[δ,54] C. Lu,[δ,55] H. Q. Lu,[δ,12] J. S. Lu,[δ,12] P. Lucas,[μ,1] K. B. Luk,[δ,49,28] X. B. Ma,[δ,20] X. Y. Ma,[δ,12] Y. Q. Ma,[δ,12] W. A. Mann,[μ,23] M. L. Marshak,[μ,31] C. Marshall,[δ,28] D. A. Martinez Caicedo,[δ,32] N. Mayer,[μ,23] K. T. McDonald,[δ,55] R. D. McKeown,[δ,56,50] R. Mehdiyev,[μ,13] J. R. Meier,[μ,31] Y. Meng,[δ,53] W. H. Miller,[μ,31] G. Mills,[μ,57,†] L. Mora Lepin,[δ,58] D. Naples,[μ,35] J. Napolitano,[δ,47] D. Naumov,[δ,22] E. Naumova,[δ,22] J. K. Nelson,[μ,50] R. J. Nichol,[μ,33] J. O'Connor,[μ,33] J. P. Ochoa-Ricoux,[δ,59] A. Olshevskiy,[δ,22] R. B. Pahlka,[μ,1] H.-R. Pan,[δ,11] J. Park,[δ,44] S. Patton,[δ,28] Ž. Pavlović,[μ,57] G. Pawloski,[μ,31] J. C. Peng,[δ,27] A. Perch,[μ,33] M. M. Pfützner,[μ,33] D. D. Phan,[μ,13] R. K. Plunkett,[μ,1] N. Poonthottathil,[μ,1] C. S. J. Pun,[δ,51] F. Z. Qi,[δ,12] M. Qi,[δ,54] X. Qian,[δ,8] X. Qiu,[μ,60] A. Radovic,[μ,50] N. Raper,[δ,19] J. Ren,[δ,42] C. Morales Reveco,[δ,58] R. Rosero,[δ,8] B. Roskovec,[δ,59] X. C. Ruan,[δ,42] P. Sail,[μ,13] M. C. Sanchez,[μ,3] J. Schneps,[μ,23,†] A. Schreckenberger,[μ,13] N. Shaheed,[δ,43] R. Sharma,[μ,1] A. Sousa,[μ,46] H. Steiner,[δ,49,28] J. L. Sun,[δ,61] N. Tagg,[μ,62] J. Thomas,[μ,33] M. A. Thomson,[μ,9] A. Timmons,[μ,16] T. Tmej,[δ,26] J. Todd,[μ,46] S. C. Tognini,[μ,14] R. Toner,[μ,29] D. Torretta,[μ,1] K. Treskov,[δ,22] W.-H. Tse,[δ,21] C. E. Tull,[δ,28] P. Vahle,[μ,50] B. Viren,[δ,8] V. Vorobel,[δ,26] C. H. Wang,[δ,15] J. Wang,[δ,19] M. Wang,[δ,43] N. Y. Wang,[δ,37] R. G. Wang,[δ,12] W. Wang,[δ,19,50] W. Wang,[δ,54] X. Wang,[δ,63] Y. Wang,[δ,54] Y. F. Wang,[δ,12] Z. Wang,[δ,12] Z. Wang,[δ,17] Z. M. Wang,[δ,12] A. Weber,[μ,7,64] H. Y. Wei,[δ,8] L. H. Wei,[δ,12] L. J. Wen,[δ,12] K. Whisnant,[δ,3] C. White,[δ,32] L. H. Whitehead,[μ,33] S. G. Wojcicki,[μ,60] H. L. H. Wong,[δ,49,28] S. C. F. Wong,[δ,19] E. Worcester,[δ,8] D. R. Wu,[δ,12] F. L. Wu,[δ,54] Q. Wu,[δ,43] W. J. Wu,[δ,12] D. M. Xia,[δ,65] Z. Q. Xie,[δ,12] Z. Z. Xing,[δ,12] J. L. Xu,[δ,12] T. Xu,[δ,17] T. Xue,[δ,17] C. G. Yang,[δ,12] L. Yang,[δ,48] Y. Z. Yang,[δ,17] H. F. Yao,[δ,12] M. Ye,[δ,12] M. Yeh,[δ,8] B. L. Young,[δ,3] H. Z. Yu,[δ,19] Z. Y. Yu,[δ,12] B. B. Yue,[δ,19] S. Zeng,[δ,12] Y. Zeng,[δ,19] L. Zhan,[δ,12] C. Zhang,[δ,8] F. Y. Zhang,[δ,53] H. H. Zhang,[δ,19] J. W. Zhang,[δ,12] Q. M. Zhang,[δ,38] X. T. Zhang,[δ,12] Y. M. Zhang,[δ,19] Y. X. Zhang,[δ,61] Y. Y. Zhang,[δ,53] Z. J. Zhang,[δ,48] Z. P. Zhang,[δ,25] Z. Y. Zhang,[δ,12] J. Zhao,[δ,12] L. Zhou,[δ,12] and H. L. Zhuang[δ,12]

(Daya Bay Collaboration)[δ]

(MINOS+ Collaboration)[μ]

[1]*Fermi National Accelerator Laboratory, Batavia, Illinois 60510, USA*
[2]*Institute of Modern Physics, East China University of Science and Technology, Shanghai*
[3]*Department of Physics and Astronomy, Iowa State University, Ames, Iowa 50011 USA*
[4]*Department of Physics, University of Cincinnati, Cincinnati, Ohio 45221, USA*
[5]*Physics Department, University of Wisconsin, Madison, Wisconsin 53706, USA*
[6]*Wright Laboratory and Department of Physics, Yale University, New Haven, Connecticut 06520, USA*
[7]*Subdepartment of Particle Physics, University of Oxford, Oxford OX1 3RH, United Kingdom*
[8]*Brookhaven National Laboratory, Upton, New York 11973, USA*

[9]Cavendish Laboratory, University of Cambridge, Cambridge CB3 0HE, United Kingdom
[10]Lancaster University, Lancaster, LA1 4YB, United Kingdom
[11]Department of Physics, National Taiwan University, Taipei
[12]Institute of High Energy Physics, Beijing
[13]Department of Physics, University of Texas at Austin, Austin, Texas 78712, USA
[14]Instituto de Física, Universidade Federal de Goiás, 74690-900, Goiânia, Goias, Brazil
[15]National United University, Miao-Li
[16]Department of Physics and Astronomy, University of Manchester, Manchester M13 9PL, United Kingdom
[17]Department of Engineering Physics, Tsinghua University, Beijing
[18]Shenzhen University, Shenzhen
[19]Sun Yat-Sen (Zhongshan) University, Guangzhou
[20]North China Electric Power University, Beijing
[21]Chinese University of Hong Kong, Hong Kong
[22]Joint Institute for Nuclear Research, Dubna, Moscow Region, Russia
[23]Physics Department, Tufts University, Medford, Massachusetts 02155, USA
[24]Siena College, Loudonville, New York 12211, USA
[25]University of Science and Technology of China, Hefei
[26]Charles University, Faculty of Mathematics and Physics, Prague, Czech Republic
[27]Department of Physics, University of Illinois at Urbana-Champaign, Urbana, Illinois 61801, USA
[28]Lawrence Berkeley National Laboratory, Berkeley, California, 94720 USA
[29]Department of Physics, Harvard University, Cambridge, Massachusetts 02138, USA
[30]Department of Physics, University of Dallas, Irving, Texas 75062, USA
[31]University of Minnesota, Minneapolis, Minnesota 55455, USA
[32]Department of Physics, Illinois Institute of Technology, Chicago, Illinois 60616, USA
[33]Department of Physics and Astronomy, University College London, London WC1E 6BT, United Kingdom
[34]Instituto de Física, Universidade de São Paulo, CP 66318, 05315-970, São Paulo, Sao Paulo, Brazil
[35]Department of Physics and Astronomy, University of Pittsburgh, Pittsburgh, Pennsylvania 15260, USA
[36]Department of Physics, University of Warsaw, PL-02-093 Warsaw, Poland
[37]Beijing Normal University, Beijing
[38]Department of Nuclear Science and Technology, School of Energy and Power Engineering, Xi'an Jiaotong University, Xi'an
[39]Department of Physics, University of Minnesota Duluth, Duluth, Minnesota 55812, USA
[40]Department of Physics and Astronomy, University of Sussex, Falmer, Brighton BN1 9QH, United Kingdom
[41]Department of Physics, University of Houston, Houston, Texas 77204, USA
[42]China Institute of Atomic Energy, Beijing
[43]Shandong University, Jinan
[44]Center for Neutrino Physics, Virginia Tech, Blacksburg, Virginia 24061, USA
[45]Institute of Physics, National Chiao-Tung University, Hsinchu
[46]Department of Physics, University of Cincinnati, Cincinnati, Ohio 45221, USA
[47]Department of Physics, College of Science and Technology, Temple University, Philadelphia, Pennsylvania 19122, USA
[48]Dongguan University of Technology, Dongguan
[49]Department of Physics, University of California, Berkeley, California 94720, USA
[50]Department of Physics, College of William & Mary, Williamsburg, Virginia 23187, USA
[51]Department of Physics, The University of Hong Kong, Pokfulam, Hong Kong
[52]School of Physics, Nankai University, Tianjin
[53]Department of Physics and Astronomy, Shanghai Jiao Tong University, Shanghai Laboratory for Particle Physics and Cosmology, Shanghai
[54]Nanjing University, Nanjing
[55]Joseph Henry Laboratories, Princeton University, Princeton, New Jersey 08544, USA
[56]Lauritsen Laboratory, California Institute of Technology, Pasadena, California 91125, USA
[57]Los Alamos National Laboratory, Los Alamos, New Mexico 87545, USA
[58]Instituto de Física, Pontificia Universidad Católica de Chile, Santiago, Chile
[59]Department of Physics and Astronomy, University of California, Irvine, California 92697, USA
[60]Department of Physics, Stanford University, Stanford, California 94305, USA
[61]China General Nuclear Power Group, Shenzhen
[62]Otterbein University, Westerville, Ohio 43081, USA
[63]College of Electronic Science and Engineering, National University of Defense Technology, Changsha

[64]Rutherford Appleton Laboratory, Science and Technology Facilities Council, Didcot, OX11 0QX, United Kingdom
[65]Chongqing University, Chongqing

(Received 4 February 2020; revised 13 June 2020; accepted 15 June 2020; published 10 August 2020)

Searches for electron antineutrino, muon neutrino, and muon antineutrino disappearance driven by sterile neutrino mixing have been carried out by the Daya Bay and MINOS+ collaborations. This Letter presents the combined results of these searches, along with exclusion results from the Bugey-3 reactor experiment, framed in a minimally extended four-neutrino scenario. Significantly improved constraints on the $\theta_{\mu e}$ mixing angle are derived that constitute the most constraining limits to date over five orders of magnitude in the mass-squared splitting Δm^2_{41}, excluding the 90% C.L. sterile-neutrino parameter space allowed by the LSND and MiniBooNE observations at 90% CL_s for $\Delta m^2_{41} < 13\ \mathrm{eV}^2$. Furthermore, the LSND and MiniBooNE 99% C.L. allowed regions are excluded at 99% CL_s for $\Delta m^2_{41} < 1.6\,\mathrm{eV}^2$.

DOI: 10.1103/PhysRevLett.125.071801

Neutrino oscillation has been confirmed by a wealth of experimental data accumulated since its discovery over two decades ago [1,2]. Neutrinos are created and absorbed in so-called weak states consisting of a coherent superposition of mass eigenstates that evolves in time, thus, the weak states at production and at a later interaction do not necessarily coincide.

Most of the measurements made so far with solar, atmospheric, reactor, and accelerator neutrinos [3–15] can be fully explained with three neutrino states that mix as described by the Pontecorvo-Maki-Nakagawa-Sakata formalism [16–18]. There are, however, some experimental observations that cannot be accommodated in the three-neutrino mixing model, such as the excess of electronlike events in a muon (anti)neutrino beam observed over short baselines by the Liquid Scintillator Neutrino Detector (LSND) [19] and MiniBooNE [20,21] experiments. These observations may be explained by mixing with at least one additional fourth neutrino state with $\Delta m^2_{41} \gg |\Delta m^2_{32}|$, where the $\Delta m^2_{ji} = m^2_j - m^2_i$ represent neutrino mass-squared differences, and m_i is the mass of the ith mass eigenstate. The addition of such states, a natural occurrence in many extensions of the standard model of particle physics that incorporate neutrino masses [22], results in new neutrino states that are commonly deemed to be sterile in accordance with the tight constraints from precision electroweak measurements [23,24] on the number of neutrinos that couple to the Z boson. The far-reaching implications of sterile neutrinos in particle physics and cosmology make their possible existence one of the key questions in physics.

Sterile neutrinos could be detected in oscillation experiments as a deviation from the standard three-neutrino oscillation behavior if they are a mixture of the fourth and other mass eigenstates. In 2016, the Daya Bay and MINOS experiments reported limits on active-to-sterile oscillations obtained by combining the results of their electron antineutrino and muon (anti)neutrino disappearance measurements, respectively [25], with those from the Bugey-3 experiment [26]. This Letter presents significantly improved limits obtained by utilizing a data set with roughly twice the exposure in the case of Daya Bay [27], and by adding 5.80×10^{20} protons-on-target (POT) of MINOS+ data, recorded with the medium-energy configuration of the NuMI beam [28], to the full MINOS data sample [29]. Some key systematic uncertainties are reduced in the case of Daya Bay, and a new two-detector fit technique is employed for MINOS and MINOS+. The resulting limits provide leading constraints on possible mixing between active and sterile neutrinos, and can be used to examine the sterile neutrino interpretation of the appearance claims made by the LSND and MiniBooNE experiments in a way that is independent of CP violation and mass-ordering effects.

The results of the combined analysis presented in this Letter are interpreted within the framework of a $3+1$ model, which includes one new mass eigenstate and one sterile weak eigenstate in addition to the three known mass eigenstates and active neutrino flavors. We parametrize the extended 4×4 unitary matrix U describing mixing between weak and mass eigenstates following Ref. [30], and the expressions for the elements of U that are relevant to this Letter become

$$\begin{aligned} |U_{e3}|^2 &= \cos^2\theta_{14}\sin^2\theta_{13}, \\ |U_{e4}|^2 &= \sin^2\theta_{14}, \\ |U_{\mu 4}|^2 &= \sin^2\theta_{24}\cos^2\theta_{14}. \end{aligned} \tag{1}$$

Under the assumption of neutrino-antineutrino invariance, in the $\Delta m^2_{41} \gg |\Delta m^2_{31}|$ approximation for Daya Bay and Bugey-3 baselines, the survival probability of electron antineutrinos with energy E after traveling a distance L approximates to

$$P_{\bar{\nu}_e\to\bar{\nu}_e} \approx 1 - 4|U_{e4}|^2(1-|U_{e4}|)^2 \sin^2\left(\frac{\Delta m^2_{41}L}{4E}\right) - 4|U_{e3}|^2(1-|U_{e3}|^2)\sin^2\left(\frac{\Delta m^2_{31}L}{4E}\right), \quad (2)$$

which yields the following $\sin^2 2\theta_{14}$-dependent expression:

$$P_{\bar{\nu}_e\to\bar{\nu}_e} \approx 1 - \sin^2 2\theta_{14}\sin^2\left(\frac{\Delta m^2_{41}L}{4E}\right) - \sin^2 2\theta_{13}\sin^2\left(\frac{\Delta m^2_{31}L}{4E}\right). \quad (3)$$

Long-baseline experiments like MINOS and MINOS+ constrain $\sin^2\theta_{24}$ by precisely measuring muon neutrino and antineutrino disappearance, for which we can approximate the survival probability as

$$P_{\overset{(-)}{\nu}_\mu\to\overset{(-)}{\nu}_e} \approx 1 - \sin^2 2\theta_{23}\cos 2\theta_{24}\sin^2\left(\frac{\Delta m^2_{31}L}{4E}\right) - \sin^2 2\theta_{24}\sin^2\left(\frac{\Delta m^2_{41}L}{4E}\right). \quad (4)$$

In addition, long-baseline experiments can also look for deficits in the rate of neutral-current (NC) neutrino interactions at the near and far detectors, approximately described by

$$\begin{aligned} P_{\mathrm{NC}} &= 1 - P(\nu_\mu\to\nu_s) \\ &\approx 1 - \cos^4\theta_{14}\cos^2\theta_{34}\sin^2 2\theta_{24}\sin^2\left(\frac{\Delta m^2_{41}L}{4E}\right) \\ &\quad - \sin^2\theta_{34}\sin^2 2\theta_{23}\sin^2\left(\frac{\Delta m^2_{31}L}{4E}\right) \\ &\quad + \frac{1}{2}\sin\delta_{24}\sin\theta_{24}\sin 2\theta_{34}\sin 2\theta_{23}\sin\left(\frac{\Delta m^2_{31}L}{2E}\right). \end{aligned} \quad (5)$$

Besides sensitivity to both θ_{24} and Δm^2_{41}, the NC channel provides sensitivity to θ_{14}, θ_{34}, and δ_{24}. (Anti)neutrino muon to electron (anti)neutrino appearance driven by a fourth mass state has been advanced as a possible explanation of the LSND and MiniBooNE results. Over a short baseline (SBL), this appearance probability is described by

$$P^{SBL}_{\overset{(-)}{\nu}_\mu\to\overset{(-)}{\nu}_e} = 4|U_{e4}|^2|U_{\mu4}|^2\sin^2\left(\frac{\Delta m^2_{41}L}{4E}\right), \quad (6)$$

where

$$4|U_{e4}|^2|U_{\mu4}|^2 = \sin^2 2\theta_{14}\sin^2\theta_{24} \equiv \sin^2 2\theta_{\mu e}. \quad (7)$$

Therefore, electron antineutrino disappearance constraints from reactors on $\sin^2 2\theta_{14}$, combined with muon neutrino and antineutrino disappearance constraints from long-baseline experiments on $\sin^2\theta_{24}$, can place strong constraints on the quadratically suppressed electron neutrino or antineutrino appearance described by $\sin^2 2\theta_{\mu e}$ within the framework of the $3+1$ model [31]. While Eqs. (3) and (4) show leading terms to illustrate the general behavior of the oscillation probabilities, exact formulas of the full survival probabilities are used in the analyses reported in this Letter.

The Daya Bay reactor antineutrino experiment consists of eight identically designed antineutrino detectors (ADs) placed in three underground experimental halls (EHs) at different distances from three pairs of 2.9 $\mathrm{GW_{th}}$ nuclear reactors in the southeast of China. The two near halls, EH1 and EH2, house two ADs each and have flux-averaged baselines on the order of 550 m. The far hall, EH3, houses four ADs and has a flux-averaged baseline around 1600 m. The overburdens of EH1, EH2, and EH3 are 250, 265, and 860 meters-water-equivalent, respectively. Electron antineutrinos are detected via the inverse beta decay (IBD) reaction, $\bar{\nu}_e + p \to e^+ + n$, whose two products are visible in the ADs. Further details about the Daya Bay experiment can be found in Ref. [32].

Daya Bay's unique configuration with multiple baselines makes it well suited to search for sterile neutrino mixing. A relative comparison of the rate and spectral shape of reactor antineutrinos observed in the EHs at different baselines provides most of the sensitivity to sterile neutrino oscillations in the $10^{-3}\ \mathrm{eV}^2 \lesssim|\Delta m^2_{41}|\lesssim 0.3\ \mathrm{eV}^2$ region. For $|\Delta m^2_{41}|\gtrsim 0.3\ \mathrm{eV}^2$, the oscillations are too fast to be resolved by the detectors, and the sensitivity arises primarily from comparing the measured rate with the expectation. The uncertainty in the expected reactor antineutrino flux is conservatively set to 5% as motivated by recent reevaluations in light of the so-called reactor antineutrino anomaly [33,34].

A new search for light sterile neutrino mixing was performed at Daya Bay with a data set acquired over 1230 days. This represents a factor of ~2 increase in exposure over the previous result [35]. The analysis of this data set incorporates other improvements, such as a more precise background assessment, the inclusion of a time-dependent correction for spatial nonuniformity within each AD, and a reduction in the relative detection efficiency uncertainty to 0.2%, which is the dominant source of systematic error. The IBD selection, background rejection, and assessment of systematic uncertainties for this data set are described in detail in Ref. [27]. The normal mass ordering is assumed for Δm^2_{31} and Δm^2_{41}. The results reported here are largely insensitive to this choice.

The same two complementary methods applied in previous sterile neutrino searches at Daya Bay [35,36] are used to set the exclusion limits in the $(\Delta m^2_{41}, \sin^2 2\theta_{14})$ parameter space. The first one is based on a purely relative comparison between the near and the far data and relies on the frequentist approach proposed by Feldman and Cousins to determine the exclusion limits [37]. In this approach, $\Delta\chi^2 = \chi^2_{\mathrm{point}} - \chi^2_{\mathrm{best\ fit}}$ distributions are generated for each $(\Delta m^2_{41}, \sin^2 2\theta_{14})$ point by fitting a large number of

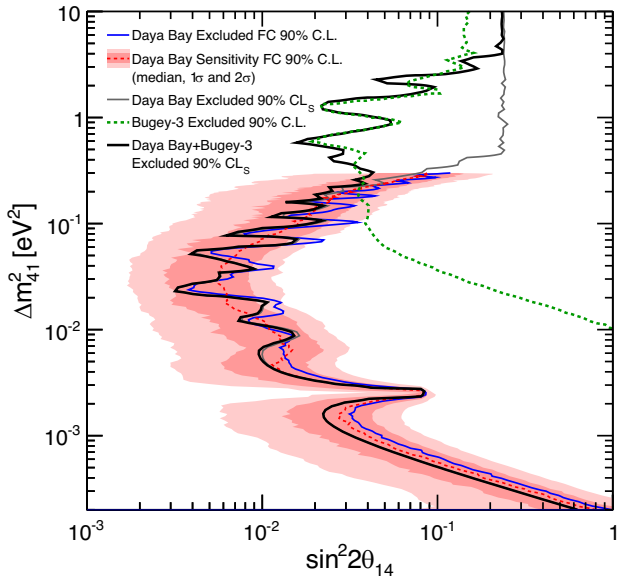

FIG. 1. The Feldman-Cousins (FC) exclusion region at 90% C.L. from the analysis of 1230 days of Daya Bay data is shown as the solid blue line. The 90% C.L. median sensitivity is shown as the dashed red line, along with 1σ and 2σ bands. The excluded region for the original Bugey-3 limit with the raster scan technique is shown in green, while the resulting CL_s contour from Daya Bay and its combination with the reproduced Bugey-3 results with adjusted fluxes are shown in grey and black, respectively. The regions to the right of the curves are excluded at the 90% CL_s or 90% C.L.

pseudoexperiments with statistical and systematic fluctuations. For each pseudoexperiment, the fit relies on both the rate and spectral shape information and involves a global minimization with Δm^2_{41}, $\sin^2 2\theta_{14}$, and $\sin^2 2\theta_{13}$ as free parameters. The resulting $\Delta\chi^2$ distribution for each point is then compared with the corresponding $\Delta\chi^2$ value obtained with the data to determine if that point is included in the exclusion contour.

The second one uses the predicted antineutrino spectra to simultaneously fit the observations in the three halls, and uses the CL_s statistical method [38,39] to set the limits. The CL_s method is a two-hypothesis test, used here to discriminate between the three-neutrino (3ν) and four-neutrino (4ν) scenarios where each combination of (Δm^2_{41}, $\sin^2 2\theta_{14}$) is treated as a separate 4ν scenario. We define the test statistic $\Delta\chi^2 = \chi^2_{4\nu} - \chi^2_{3\nu}$, where $\chi^2_{3\nu}$ is the minimum χ^2 in a fit to the 3ν hypothesis (with free θ_{13}) and $\chi^2_{4\nu}$ is the minimum χ^2 in a fit to the 4ν hypothesis (with free θ_{13}, and Δm^2_{41} and θ_{14} set to the corresponding 4ν scenario under consideration). The fits rely on both the rate and spectral shape information. Other parameters, namely $\sin^2 2\theta_{12}$, Δm^2_{21}, and $|\Delta m^2_{32}|$, are constrained using external data [23]. We produce a $\Delta\chi^2_{3\nu}$ distribution by fitting simulated pseudoexperiments with $\Delta m^2_{41} = \sin^2 2\theta_{14} = 0$ and θ_{13} fixed to the best-fit value in the data. The same is done to construct a $\Delta\chi^2_{4\nu}$ distribution for every point in the (Δm^2_{41}, $\sin^2 2\theta_{14}$) parameter space. Since the $\Delta\chi^2_{3\nu}$ and $\Delta\chi^2_{4\nu}$ distributions are normally distributed, we estimate their mean and variance from Asimov data sets [40], greatly reducing the amount of computation needed. For each point in (Δm^2_{41}, $\sin^2 2\theta_{14}$) the observed $\Delta\chi^2_{\mathrm{obs}}$ is compared to the $\Delta\chi^2_{3\nu}$ and $\Delta\chi^2_{4\nu}$ distributions in order to obtain the corresponding p-values. The CL_s statistic is defined by

$$\mathrm{CL}_s = \frac{1 - p_{4\nu}}{1 - p_{3\nu}}, \tag{8}$$

where p_H is the p-value for hypothesis H. The 90% exclusion contour is obtained by requiring $\mathrm{CL}_s \leq 0.1$.

As seen in Fig. 1, consistent results are obtained by the two methods. It has been shown that the CL_s approach can yield more constraining exclusion contours than the Feldman-Cousins approach with null data sets [40]. Moreover, a study using a very large number of simulated experiments found that the purely relative near-far comparison method that is used to produce the Feldman-Cousins contours had slightly lower sensitivity in the $\Delta m^2_{41} \lesssim 2 \times 10^{-3}$ eV^2 region than the method where the near and far observations are fit simultaneously. This study also found that the two methods can react slightly differently to statistical fluctuations. Thus, the small differences observed in Fig. 1 are well within expectation.

A CL_s-based analysis is also applied to the published data from the Bugey-3 experiment [26]. This reactor experiment operated at shorter (< 100 m) baselines, allowing it to provide valuable constraints on sterile neutrino mixing from electron antineutrino disappearance for higher values of Δm^2_{41} compared to Daya Bay. The same methodology detailed in Ref. [25] was followed to generate the exclusion contour for Bugey-3. The main adjustments made with respect to the original Bugey-3 analysis were (i) the use of the Gaussian CL_s method, instead of the raster scan technique, (ii) the use of an updated neutron lifetime in the IBD cross-section calculation, and (iii) the use of the Huber + Mueller [41,42] model, instead of the original ILL + Vogel model [43,44], to make the flux prediction at the different baselines. The reproduced contour is very similar to the one published originally by the Bugey-3 collaboration, shown in Fig. 1.

The MINOS and MINOS+ experiments used two detectors placed on the NuMI beam axis, the near detector (ND), located 1.04 km downstream from the production target at Fermilab at a depth of 225 meters-water-equivalent, and the far detector (FD), located 734 km further downstream, in the Soudan Underground Laboratory in Minnesota at a depth of 2070 meters-water-equivalent. The detectors were functionally identical magnetized, tracking, sampling calorimeters composed of steel-scintillator planes read out by multianode photomultiplier tubes [45]. The NuMI neutrino beam is produced by impinging 120 GeV protons accelerated by the Main Injector complex at Fermilab onto a graphite target. The emerging secondary beam of mostly π and K mesons is focused by two parabolic electromagnetic horns and allowed

to decay in a 675 m long helium-filled pipe, resulting in a neutrino beam composed predominantly of ν_μ, with a 1.3% contamination of ν_e [46]. The detectors accumulated a 10.56×10^{20} POT beam exposure during the MINOS neutrino runs, with the observed neutrino energy spectrum peaked at 3 GeV. In the MINOS+ phase, the detectors sampled a higher-intensity NuMI beam, upgraded as part of the NOvA experiment [47], with the neutrino energy spectrum peaked at 7 GeV. The higher-energy neutrino beam, although less favorable for three-flavor oscillation measurements (for MINOS' baseline and three-neutrino standard oscillations, the muon neutrino disappearance maximum occurs at $E_\nu \approx 1.6$ GeV), provides greater sensitivity to sterile-induced muon neutrino disappearance by increasing the statistics in regions of L/E_ν where oscillations driven by large mass-squared splittings would occur. A new search for sterile neutrino mixing using an additional exposure of 5.80×10^{20} POT of MINOS+ data has been recently published [29]. Unlike the previous MINOS analysis based on the ratio between the measured neutrino energy spectra in the two detectors (far-over-near ratio) [48–51], limited by the statistical error of the lower-statistics FD sample, the new analysis employs a two-detector fit method, simultaneously fitting the reconstructed neutrino energy spectra in both detectors [52]. The new technique exploits the full power of the large ND statistics for L/E_ν regions probed by the ND baseline.

The analysis employs both the charged-current (CC) ν_μ and the NC data samples from MINOS and MINOS+. The CC ν_μ disappearance channel has sensitivity to θ_{24} and Δm^2_{41}, in addition to the three-flavor oscillation parameters Δm^2_{32} and θ_{23}. The NC sample has sensitivity to θ_{34}, θ_{24}, and Δm^2_{41}, albeit with a worse energy resolution (due to the missing energy carried by the outgoing final-state neutrino) than in the CC case, as well as lower statistics due to the lower NC interaction cross section. As detailed in Refs. [29,52], the analysis is approximately independent of the angle θ_{14} and the phases δ_{13}, δ_{14}, and δ_{24}, so these parameters are all set to zero in the fit. The MINOS and MINOS+ combined search for sterile neutrinos places the most constraining limit to date on the mixing parameter $\sin^2\theta_{24}$ for most values of the sterile neutrino mass-splitting $\Delta m^2_{41} > 10^{-4}$ eV^2.

Following the same approach used in the first joint analysis by MINOS and Daya Bay [25], the CL$_s$ contours for the new two-detector fit of MINOS and MINOS+ data are obtained using a similar prescription to the one used by Daya Bay, but where the test statistics $\Delta\chi^2_{3\nu}$ and $\Delta\chi^2_{4\nu}$ are approximated by MC simulations of pseudoexperiments without assuming they have Gaussian distributions. The consistency with the published Feldman-Cousins corrected limits is displayed in Fig. 2. The new MINOS and MINOS+ limits are combined with the Daya Bay and Bugey-3 limits described above to obtain a new improved limit on anomalous ν_μ to ν_e oscillations, as discussed below.

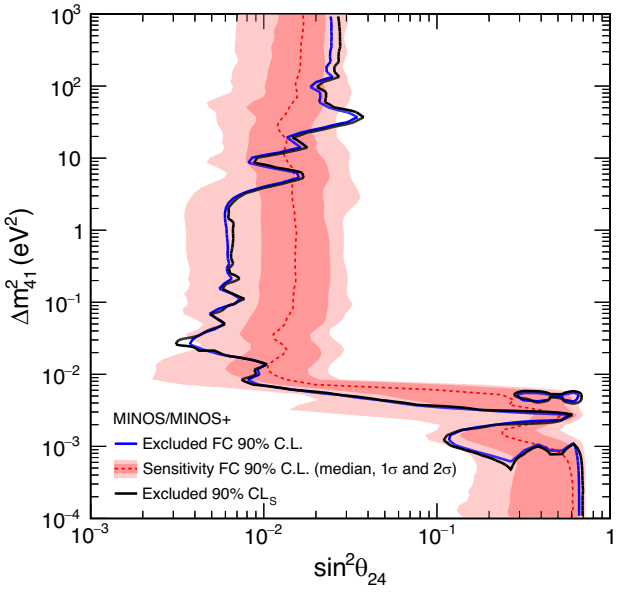

FIG. 2. Comparison of the MINOS and MINOS+ 90% C.L. exclusion contour using the Feldman-Cousins method [53] and the CL$_s$ method. The regions to the right of the curves are excluded at the 90% C.L. (CL$_s$). The 90% C.L. median sensitivity is shown in red along with the 1σ and 2σ bands.

The disappearance measurements from the three experiments are combined using the same methodology as in Ref. [25]. For each fixed value of Δm^2_{41}, the $\Delta\chi^2_{\text{obs}}$ value and the $\Delta\chi^2_{3\nu}$ and $\Delta\chi^2_{4\nu}$ distributions for each ($\sin^2 2\theta_{14}$, Δm^2_{41}) point from the Daya Bay and Bugey-3 combination are paired with those for each ($\sin^2\theta_{24}$, Δm^2_{41}) point from the MINOS and MINOS+ experiments, resulting in specific ($\sin^2 2\theta_{\mu e}$, Δm^2_{41}) combinations according to Eq. (7). Since systematic uncertainties of accelerator and reactor experiments are largely uncorrelated, the combined values of $\Delta\chi^2_{\text{obs}}$ are obtained by simply summing the corresponding values from the reactor and accelerator experiments. Similarly, the combined $\Delta\chi^2_{3\nu}$ and $\Delta\chi^2_{4\nu}$ distributions are calculated by random sampling the distributions from each experiment and summing. Since several different combinations of ($\sin^2 2\theta_{14}$, $\sin^2\theta_{24}$) can yield the same $\sin^2 2\theta_{\mu e}$, the combination with the largest CL$_s$ value is selected to be used in the final result. The CL$_s$ surfaces for Daya Bay and Bugey-3, MINOS and MINOS+, and their combination, are available in the Supplemental Material [54].

The new combined 90% and 99% CL$_s$ limits from searches for sterile neutrino mixing in MINOS, MINOS+, Daya Bay, and Bugey-3 in the $3+1$ neutrino model are shown in Figs. 3 and 4, respectively. Constraints on the $\sin^2 2\theta_{\mu e}$ electron (anti)neutrino appearance parameter are provided over 7 orders of magnitude in the mass-squared splitting Δm^2_{41}. These limits are the world's most constraining over 5 orders of magnitude, for $\Delta m^2_{41} \lesssim 10$ eV^2.

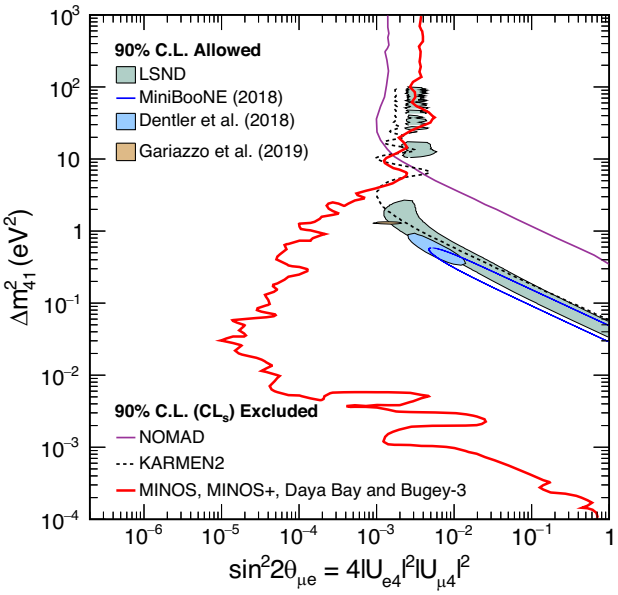

FIG. 3. Comparison of the MINOS, MINOS+, Daya Bay, and Bugey-3 combined 90% CL$_s$ limit on sin^2 $2\theta_{\mu e}$ to the LSND and MiniBooNE 90% C.L. allowed regions. Regions of parameter space to the right of the red contour are excluded. The regions excluded at 90% C.L. by the KARMEN2 Collaboration [55] and the NOMAD Collaboration [56] are also shown. The combined limit also excludes the 90% C.L. region allowed by a fit to global data by Gariazzo *et al.* where MINOS, MINOS+, Daya Bay, and Bugey-3 are not included [57,58], and the 90% C.L. region allowed by a fit to all available appearance data by Dentler *et al.* [59] updated with the 2018 MiniBooNE appearance results [21].

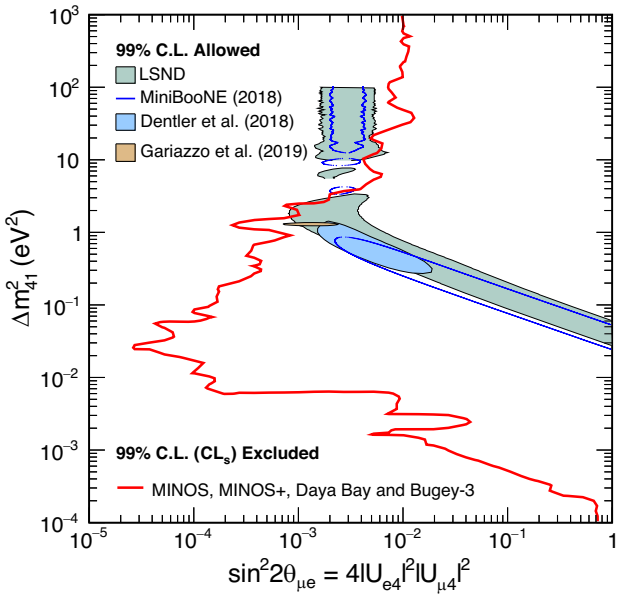

FIG. 4. Comparison of the MINOS, MINOS+, Daya Bay, and Bugey-3 combined 99% CL$_s$ limit on sin^2 $2\theta_{\mu e}$ to the LSND and MiniBooNE 99% C.L. allowed regions. The limit also excludes the 99% C.L. region allowed by a fit to global data by Gariazzo *et al.* where MINOS, MINOS+, Daya Bay, and Bugey-3 are not included [57,58], and the 99% C.L. region allowed by a fit to all available appearance data by Dentler *et al.* [59] updated with the 2018 MiniBooNE appearance results [21].

The new constraints exclude the entire 90% C.L. allowed regions from LSND and MiniBooNE for $\Delta m^2_{41} < 13$ eV^2, with regions at higher values being excluded by NOMAD [56]. Further, the 99% C.L. allowed regions from LSND and MiniBooNE are excluded for $\Delta m^2_{41} < 1.6$ eV^2. The allowed region from a global fit to data from sterile neutrino probes, intentionally excluding MINOS, MINOS+, Daya Bay, and Bugey-3 contributions, computed by the authors of Refs. [57,58], is fully excluded at the 99% C.L. The allowed region resulting from a fit to all appearance data, updated by the authors of Ref. [59] to include the MiniBooNE 2018 results [21], is equally strongly excluded. Thus, the new limits presented here significantly increase the tension between pure sterile neutrino mixing explanations of appearance-based indications and the null results from disappearance searches. The sole consideration of additional sterile neutrino states cannot resolve this tension, which stems from the nonobservation of $\bar{\nu}_e$ and $\overset{(-)}{\nu}_\mu$ disappearance beyond what is expected from the three-neutrino mixing model. This inconsistency may be further quantified in additional detector exposures in the process of being analyzed, specifically the last year of MINOS+ data taking, representing an additional sample of similar size to the one used here, as well as over two more years of Daya Bay data.

We gratefully acknowledge valuable contributions by Carlo Giunti, for supplying a custom fit to global data excluding MINOS, MINOS+, Daya Bay, and Bugey-3 data, and by Mona Dentler and Joachim Kopp, for providing an updated version of a fit to global appearance data including information from the 2018 MiniBooNE appearance results.

The Daya Bay experiment is supported in part by the Ministry of Science and Technology of China, the U.S. Department of Energy, the Chinese Academy of Sciences, the CAS Center for Excellence in Particle Physics, the National Natural Science Foundation of China, the Guangdong provincial government, the Shenzhen municipal government, the China General Nuclear Power Group, the Research Grants Council of the Hong Kong Special Administrative Region of China, the Ministry of Education in Taiwan, the U.S. National Science Foundation, the Ministry of Education, Youth and Sports of the Czech Republic, the Joint Institute of Nuclear Research in Dubna, Russia, and the National Research and Development Agency of Chile. We acknowledge Yellow River Engineering Consulting Co., Ltd. and China Railway 15th Bureau Group Co., Ltd. for building the underground laboratory. We are grateful for the ongoing cooperation from the China Guangdong Nuclear Power Group and China Light & Power Company.

The MINOS and MINOS+ Collaborations use the resources of the Fermi National Accelerator Laboratory (Fermilab), a U.S. Department of Energy, Office of Science, HEP User Facility. Fermilab is managed by Fermi Research Alliance, LLC (FRA), acting under Contract No. DE-AC02-07CH11359. This work was supported by the U.S. DOE; the United Kingdom STFC, part of UKRI; the U.S. NSF; the State and University of Minnesota; and Brazil's FAPESP, CNPq and CAPES. We thank the personnel of Fermilab's Accelerator and Scientific Computing Divisions and the crew of the Soudan Underground Laboratory for their effort and dedication. We thank the Texas Advanced Computing Center at The University of Texas at Austin for the provision of computing resources. The MINOS and MINOS+ Collaborations acknowledge fruitful cooperation with the Minnesota DNR.

[*]Now at Department of Chemistry and Chemical Technology, Bronx Community College, Bronx, New York 10453, USA.

[†]Deceased.

[1] Y. Fukuda *et al.* (Super-Kamiokande Collaboration), Phys. Rev. Lett. **81**, 1562 (1998).
[2] Q. R. Ahmad *et al.* (SNO Collaboration), Phys. Rev. Lett. **87**, 071301 (2001).
[3] B. Aharmim *et al.* (SNO Collaboration), Phys. Rev. C **88**, 025501 (2013).
[4] K. Abe *et al.* (Super-Kamiokande Collaboration), Phys. Rev. D **94**, 052010 (2016).
[5] K. Abe *et al.* (Super-Kamiokande Collaboration), Phys. Rev. D **97**, 072001 (2018).
[6] M. G. Aartsen *et al.* (IceCube Collaboration), Phys. Rev. Lett. **120**, 071801 (2018).
[7] A. Gando *et al.* (KamLAND Collaboration), Phys. Rev. D **88**, 033001 (2013).
[8] D. Adey *et al.* (Daya Bay Collaboration), Phys. Rev. Lett. **121**, 241805 (2018).
[9] G. Bak *et al.* (RENO Collaboration), Phys. Rev. Lett. **121**, 201801 (2018).
[10] Y. Abe *et al.* (Double Chooz Collaboration), J. High Energy Phys. 01 (2016) 163.
[11] K. Abe *et al.* (T2K Collaboration), Phys. Rev. Lett. **121**, 171802 (2018).
[12] M. A. Acero *et al.* (NOvA Collaboration), Phys. Rev. D **98**, 032012 (2018).
[13] P. Adamson *et al.* (MINOS Collaboration), Phys. Rev. Lett. **110**, 251801 (2013).
[14] P. Adamson *et al.* (MINOS Collaboration), Phys. Rev. Lett. **112**, 191801 (2014).
[15] N. Agafonova *et al.* (OPERA Collaboration), Phys. Rev. Lett. **120**, 211801 (2018).
[16] B. Pontecorvo, Sov. Phys. JETP **6**, 429 (1957).
[17] B. Pontecorvo, Sov. Phys. JETP **26**, 984 (1968).
[18] Z. Maki, M. Nakagawa, and S. Sakata, Prog. Theor. Phys. **28**, 870 (1962).
[19] A. Aguilar *et al.* (LSND Collaboration), Phys. Rev. D **64**, 112007 (2001).
[20] A. Aguilar-Arevalo *et al.* (MiniBooNE Collaboration), Phys. Rev. Lett. **110**, 161801 (2013).
[21] A. A. Aguilar-Arevalo *et al.* (MiniBooNE Collaboration), Phys. Rev. Lett. **121**, 221801 (2018).
[22] A. Merle, in *Sterile Neutrino Dark Matter* (Morgan & Claypool Publishers, San Rafael, Bristol, 2017), Vol. 2053, pp. 2–1–2-11, https://doi.org/10.1088/978-1-6817-4481-0ch2.
[23] K. Olive *et al.* (Particle Data Group), Chin. Phys. C **38**, 090001 (2014).
[24] S. Schael *et al.* (ALEPH Collaboration, DELPHI Collaboration, L3 Collaboration, OPAL Collaboration, SLD Collaboration, LEP Electroweak Working Group, SLD Electroweak Group, SLD Heavy Flavour Group), Phys. Rep. **427**, 257 (2006).
[25] P. Adamson *et al.* (MINOS and Daya Bay Collaborations), Phys. Rev. Lett. **117**, 151801 (2016); **117**, 209901 (2016).
[26] B. Achkar *et al.* (Bugey-3 Collaboration), Nucl. Phys. **B434**, 503 (1995).
[27] F. P. An *et al.* (Daya Bay Collaboration), Phys. Rev. D **95**, 072006 (2017).
[28] P. Adamson *et al.* (MINOS Collaboration), Nucl. Instrum. Methods Phys. Res., Sect. A **806**, 279 (2016).
[29] P. Adamson *et al.* (MINOS+ Collaboration), Phys. Rev. Lett. **122**, 091803 (2019).
[30] H. Harari and M. Leurer, Phys. Lett. B **181**, 123 (1986).
[31] S. Gariazzo, C. Giunti, M. Laveder, Y. F. Li, and E. M. Zavanin, J. Phys. G **43**, 033001 (2016).
[32] F. P. An *et al.* (Daya Bay Collaboration), Nucl. Instrum. Methods Phys. Res., Sect. A **811**, 133 (2016).
[33] A. C. Hayes, J. L. Friar, G. T. Garvey, G. Jungman, and G. Jonkmans, Phys. Rev. Lett. **112**, 202501 (2014).
[34] P. Vogel, arXiv:1603.08990.
[35] F. P. An *et al.* (Daya Bay Collaboration), Phys. Rev. Lett. **117**, 151802 (2016).
[36] F. An *et al.* (Daya Bay Collaboration), Phys. Rev. Lett. **113**, 141802 (2014).
[37] G. J. Feldman and R. D. Cousins, Phys. Rev. D **57**, 3873 (1998).
[38] A. L. Read, J. Phys. G **28**, 2693 (2002).
[39] T. Junk, Nucl. Instrum. Methods Phys. Res., Sect. A **434**, 435 (1999).
[40] X. Qian, A. Tan, J. J. Ling, Y. Nakajima, and C. Zhang, Nucl. Instrum. Methods Phys. Res., Sect. A **827**, 63 (2016).
[41] P. Huber, Phys. Rev. C **84**, 024617 (2011); **85**, 029901(E) (2012).
[42] T. A. Mueller *et al.*, Phys. Rev. C **83**, 054615 (2011).
[43] K. Schreckenbach, G.Colvin, W.Gelletly, and F. Von Feilitzsch, Phys. Lett. **160B**, 325 (1985).
[44] P. Vogel, Phys. Rev. D **29**, 1918 (1984).
[45] D. G. Michael *et al.* (MINOS Collaboration), Nucl. Instrum. Methods Phys. Res., Sect. A **596**, 190 (2008).
[46] P. Adamson *et al.*, Nucl. Instrum. Methods Phys. Res., Sect. A **806**, 279 (2016).
[47] D. S. Ayres *et al.* (NOvA Collaboration), The NOvA Technical Design Report, United States, 2007.
[48] P. Adamson *et al.* (MINOS Collaboration), Phys. Rev. Lett. **117**, 151803 (2016).
[49] P. Adamson *et al.* (MINOS Collaboration), Phys. Rev. Lett. **107**, 011802 (2011).

[50] P. Adamson *et al.* (MINOS Collaboration), Phys. Rev. D **81**, 052004 (2010).
[51] P. Adamson *et al.* (MINOS Collaboration), Phys. Rev. Lett. **101**, 221804 (2008).
[52] J. R. Todd, Ph.D. Thesis, University of Cincinnati, 2018.
[53] P. Adamson *et al.* (MINOS Collaboration), Phys. Rev. Lett. **117**, 151803 (2016).
[54] See the Supplemental Material at http://link.aps.org/supplemental/10.1103/PhysRevLett.125.071801 containing the CL_s maps from Daya Bay & Bugey-3 (Δm^2_{41} vs $\sin^2 2\theta_{14}$), MINOS & MINOS+ (Δm^2_{41} vs $\sin^2\theta_{24}$), and their combination (Δm^2_{41} vs $\sin^2 2\theta_{\mu e}$).
[55] B. Armbruster *et al.* (KARMEN Collaboration), Phys. Rev. D **65**, 112001 (2002).
[56] P. Astier *et al.* (NOMAD Collaboration), Phys. Lett. B **570**, 19 (2003).
[57] S. Gariazzo, C. Giunti, M. Laveder, and Y. F. Li, J. High Energy Phys. 06 (2017) 135.
[58] S. Gariazzo, C. Giunti, M. Laveder, and Y. F. Li, Phys. Lett. B **782**, 13 (2018).
[59] M. Dentler, A. Hernández-Cabezudo, J. Kopp, P. A. N. Machado, M. Maltoni, I. Martinez-Soler, and T. Schwetz, J. High Energy Phys. 08 (2018) 010.